

Initial Life Test of Silicone Encapsulated FR4 Printed Circuit Boards for Pre-Clinical Active Implants

Ishpa Ali^{†1}, Fei Xue^{†1}, Carlos Perez Henriquez^{†1}, Thomas Niederhoffer¹, Ahmad Shah Idil¹, Dai Jiang², & Henry T. Lancashire^{*1}

¹Department of Medical Physics and Biomedical Engineering, University College London, WC1E 6BT, London, UK.

²Department of Electronic and Electrical Engineering, University College London, WC1E 7JE, London, UK.

email: * h.lancashire@ucl.ac.uk

Abstract—Silicone encapsulated FR4 printed circuit boards may provide a rapid solution for protecting pre-clinical prototype implant electronics. Interdigitated electrodes (IDEs) with and without solder coating were manufactured on Cu-FR4 laminates and silicone encapsulated (N = 14). IDEs were aged in saline and change in impedance was measured. Solder coated IDEs had stable 1 kHz impedances throughout the aging period with promising lifetimes for pre-clinical prototypes. A single uncoated IDE failed with a fall in impedance and verdigris. Other uncoated IDEs showed increasing impedance and dark copper(II) oxide. Failures attributable to contaminants and moisture ingress are under investigation.

Keywords— life test, encapsulation, printed circuit board, impedance, FR4, solder.

I. INTRODUCTION

Pre-clinical prototype active medical implants for in vitro or animal investigations require miniaturisation, low cost, and rapid solutions for connectors [1], cables, electrode arrays, and printed circuit boards (PCBs). For clinical use active implant electronics must be protected from moisture in the body which can cause corrosion and eventual electronic failure [2]. Hermetic encapsulation with airtight packages made from metals, ceramics, and glasses is commonly used to achieve reliability over long implantation times due to their low gas permeability [3,4]. Non-hermetic polymer encapsulation is an attractive alternative to hermetic packages for prototype preclinical implants. Silicone rubber encapsulation shows high longevity for packaging circuits formed of hermetically packaged components [2], dependent upon the silicone-substrate adhesion, cleanliness, and void-free encapsulation [5,6]. Good silicone adhesion has been achieved to alumina ceramic substrates. To accelerate active implant innovation, it would be valuable to use prototype PCBs in pre-clinical studies including traditional glass-fibre-reinforced epoxy laminate (FR4) materials [7]. Promising lifetimes for silicone encapsulated FR4 PCB implants have been demonstrated [7,8]. FR4-silicone adhesion appears promising under accelerated aging with mean time to failure of 25 days at 100°C in simulated gastric fluid, extrapolated to almost 6 years at 37°C, although FR4 underperforms compared with a ceramic substrate [9]. Despite promising adhesion results we have observed corrosion at metal on FR4 surfaces within aged active implants: Fig. 1 shows copper corrosion and verdigris under silicone observed on an implant immersed in saline and continually operated for 15 days at 100°C and then stored in saline at 21°C for 8 months, corrosion was observed following the 8-month period. We hypothesise that, despite void-free silicone encapsulation, moisture can condense at the Cu-FR4 interface leading to corrosion. This paper investigates the

performance of silicone encapsulation of Cu-FR4 PCB prototypes under accelerated aging conditions.

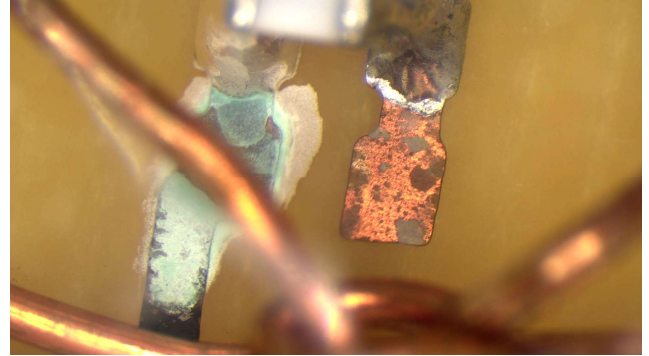


Fig. 1. Corrosion and verdigris observed on a silicone encapsulated Cu-FR4 laminate PCB in a prototype active device following accelerated aging in saline.

II. MATERIALS AND METHOD

A. Materials

Cu-FR4 laminates were acquired from Holders Technology Medical grade silicone (MED-6015) was acquired from Avantor-NuSil. MED-6015 was chosen due to its low viscosity and promising performance as an encapsulant for integrated circuits. Polishing paper up to P1200 was acquired from Agar Scientific. Solder with water soluble flux (HYDX 60EN, Multicore/Locktite), and additional water soluble flux were used (ORH1, CW8300, Chemtronics). Phosphate buffered saline was prepared from deionized water ($\geq 13 \text{ M}\Omega\cdot\text{cm}$) and tablets (Sigma Aldrich) to give pH = 7.4.

B. Sample Preparation

Copper interdigitated electrodes (IDEs) were produced from 0.8 mm thickness Cu-FR4 laminates by photolithography and wet etching. IDEs are coplanar electrode pairs between which impedance or leakage current may be measured. IDE dimensions were: 40 mm \times 0.3 mm interdigitated tracks; 9 interdigitations per electrode; 0.3 mm inter-track spacing; and 50 mm \times 15 mm outer dimensions, Fig. 2. A surrounding shield conductor was used in addition to the IDE electrode pair. IDEs were not solder mask coated, leaving conductive copper tracks exposed, Fig. 2. IDEs were either solder coated, or uncoated copper (n=6 and n=8 respectively). Prior to solder coating copper samples were cleaned by burnishing with polishing paper. All samples were soldered to silicone coated stranded copper wire at test pads. Immediately following soldering samples were cleaned in warm deionized water to remove flux. All samples were cleaned by ultrasonication in a detergent (Teepol-L) and sodium phosphate solution [6,9,10], followed by further

[†] These authors contributed equally to this work.

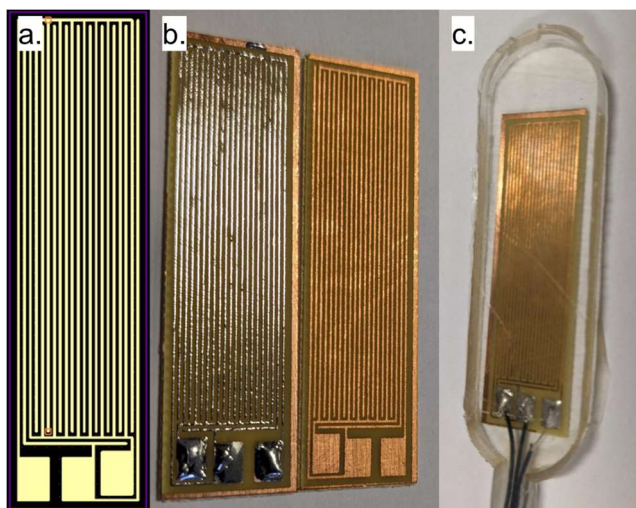


Fig. 2. a) The interdigitated electrode design. b) As produced interdigitated electrodes with (left) and without (right) solder coating. c) Silicone encapsulated interdigitated electrode.

ultrasonication in deionized water, acetone, and isopropyl alcohol. Samples were rinsed with deionized water, and cleanliness was accepted at conductivities less than 120 nS.cm^{-1} . Connecting wires were surrounded with a silicone tube which was embedded into the silicone encapsulation at the sample end [11]. Immediately prior to encapsulation sample surfaces were cleaned with air plasma for 2 minutes at 0.5 mBar. Cleaned IDEs were encapsulated with medical grade silicone by centrifuge vacuum moulding to ensure conformal, void-free, coating of the sample surface [1]. Silicone was cured at 80°C for at least 4 hours to ensure complete curing. Connecting wires were soldered to PEEK bungs and exposed metal surfaces were protected with room-temperature-vulcanizing silicone as previously described [11].

C. Sample Aging

Silicone encapsulated IDEs were aged at 21°C and 67°C in phosphate buffered saline in a previously developed accelerated ageing and life-test apparatus [11]. Changes in aging temperature were due to equipment availability. Solder coated IDEs were observed for up to 330 days, and uncoated Cu IDEs were observed for up to 222 days. Solder coated IDEs (and uncoated sample 2) were initially aged at 67°C for 1 month, followed by: 86 days not in saline; 194 days aging at 21°C ; and 1 month at 67°C . Uncoated Cu IDEs (except sample 2) were initially aged for 194 days at 21°C followed by 1 month at 67°C .

D. Electrochemical Impedance Spectroscopy

Electrical impedance spectroscopy (EIS) was repeated regularly during aging. EIS was carried out with either a Wayne-Kerr 6500B Impedance Analyser during 21°C aging or a Solartron Modulab XM potentiostat and frequency response analyser during 67°C aging. EIS was carried out from 20 Hz to 10 kHz with $50 \text{ mV}_{\text{p-p}}$ excitation amplitude with the WK6500B, and from 10 mHz to 100 kHz with $50 \text{ mV}_{\text{p-p}}$ excitation with the Modulab XM.

E. Moisture Absorption

The moisture absorption of Cu-FR4 laminate IDEs and silicone encapsulated IDEs was measured by change in mass. Dried samples ($n = 5$) were placed in deionized water at 21°C , change in mass was measured at intervals, sample surfaces

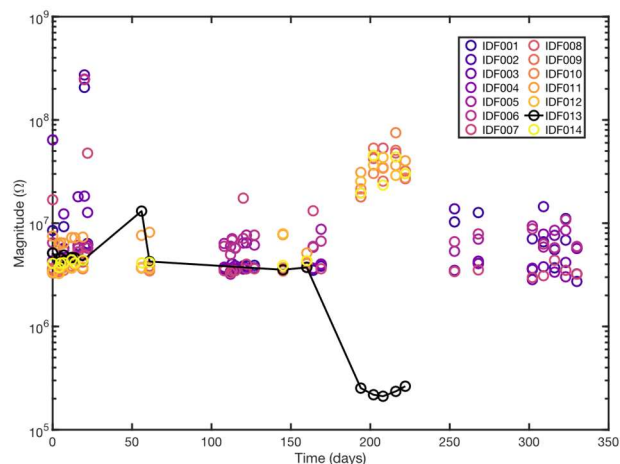


Fig. 3. 1 kHz Impedance change with time for solder coated (ID001 and 003 to 007) and uncoated (ID002 and 008 to 014) Cu-FR4 interdigitated electrodes with silicone encapsulation.

were dried using a lint-free cloth to remove surface water prior to each measurement. Sample dry mass was measured following drying in a conventional oven followed by a vacuum oven for at least 2 hours.

F. Data Analysis

Impedance at 1 kHz was calculated for all samples throughout the measurement period for comparison. Where given data are mean \pm standard deviation.

III. RESULTS

A. Impedance Changes

Change in 1kHz impedance with time is plotted in Fig. 3. Solder coated IDEs were observed to have a stable 1 kHz impedance throughout the aging period, whether aged at 21°C or 67°C . Initial 1 kHz impedance was $4.45 \pm 1.34 \text{ M}\Omega$, after 330 days 1 kHz impedance was $4.94 \pm 1.34 \text{ M}\Omega$.

For uncoated Cu IDEs 1 kHz impedances were relatively constant during aging at 21°C for 194 days. Initial 1 kHz impedance was $4.36 \pm 1.52 \text{ M}\Omega$. Following aging at 67°C

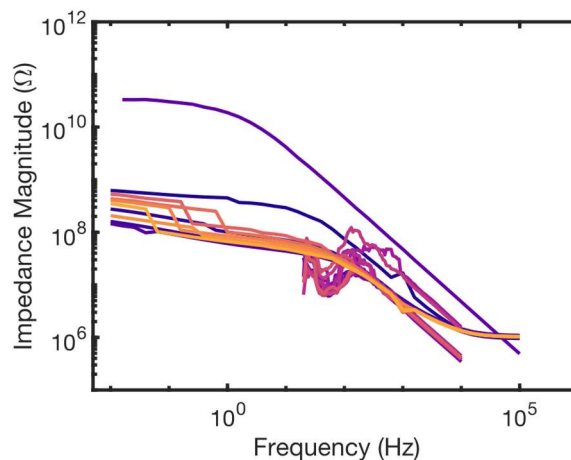


Fig. 4. Example impedance spectrum from a single solder coated Cu-FR4 interdigitated electrode (ID007). Time increase is shown as change from darker (purple) to lighter (orange). Measurements made with WK6500B have a narrower frequency range.

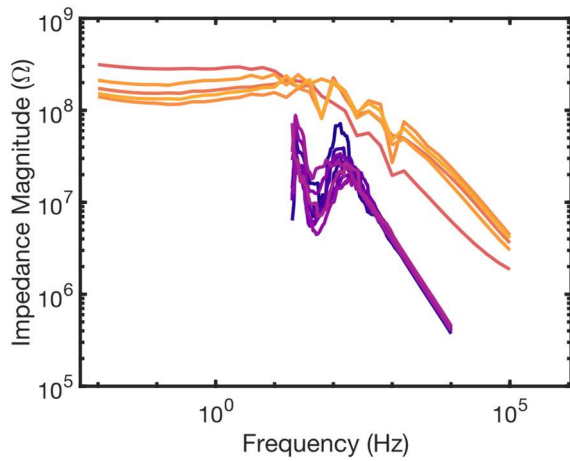


Fig. 5. Example impedance spectrum from a single uncoated Cu-FR4 interdigitated electrode (ID008). Time increase is shown as change from darker (purple) to lighter (orange). Measurements made with WK6500B have a narrower frequency range.

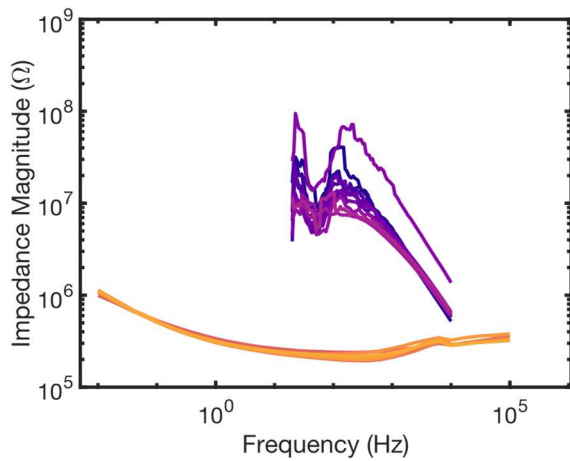


Fig. 6. Impedance spectrum from ID013 showing impedance decrease with increasing time (from darker purple to lighter orange). Measurements made with WK6500B have a narrower frequency range.



Fig. 7. Micrograph of bright surface on a solder coated Cu-FR4 interdigitated electrode with silicone encapsulation following aging. Imaged at $6.4\times$ magnification.

changes in uncoated Cu IDE impedance were observed: for most of the sample impedances were observed to increase to $31.2 \pm 4.81 \text{ M}\Omega$ after 222 days total aging; however, for a single sample impedance was observed to decrease to $264 \text{ k}\Omega$ at 222 days.

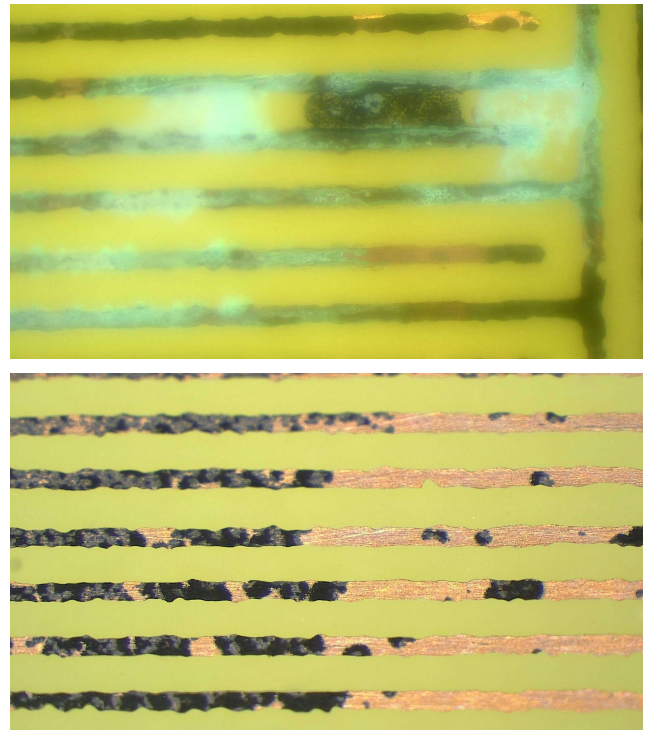


Fig. 8. Micrographs of uncoated Cu-FR4 interdigitated electrodes with silicone encapsulation. Above, ID013 with verdigris and precipitation at the FR4-silicone interface. Below, dark copper(II) oxide discoloration on the copper surface. Imaged at $16\times$ magnification.

Example impedance spectra are given for solder coated (Fig. 4) and uncoated (Fig. 5) IDEs which were observed to be representative of the respective groups. At high frequency impedance was observed to fall with increasing frequency, representative of the IDE capacitance. Low frequency impedance for both sample types was observed to plateau at $>100 \text{ M}\Omega$, this plateau was not observed with WK6500B measurements due to the instrument minimum frequency, and noisy spectra due to accuracy at high impedance / low current. The solder coated IDE spectrum showed a high frequency plateau when measured during 67°C aging, which was not observed in the limited frequency range during 21°C measurements. No clear difference in solder coated IDE impedance was observed between impedances at 1 kHz measured using different instruments. Uncoated sample 1 kHz impedance measured during 67°C aging (with Modulab XM) was approximately 1 order of magnitude greater than measured at 21°C (with WK6500B).

The impedance spectrum of the single uncoated IDE which was observed to decrease during aging is shown in Fig. 6. Impedance at low frequency was observed to fall with time during 21°C aging. All spectra recorded during 67°C aging were more representative of a resistive response, with constant phase element-like response at low frequencies and a possible inductive contribution at high frequencies.

B. Sample Observations

Solder coated IDEs were observed to have bright solder throughout the aging period, Fig. 7; however, surrounding regions of uncoated copper, not forming part of the IDE, were observed to have dark discolorations attributable to copper(II) oxide.

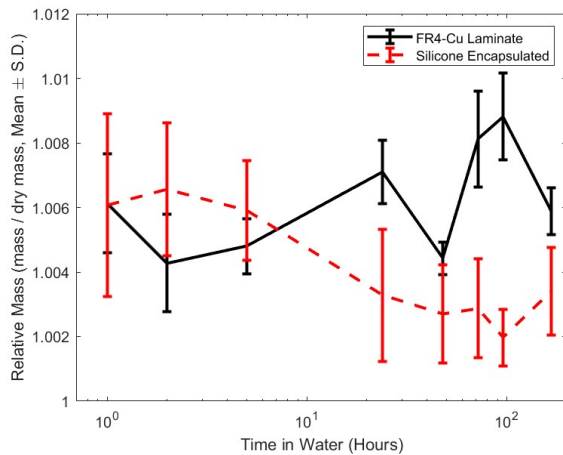


Fig. 9. Relative mass over time in deionized water for FR4-Cu laminate and silicone encapsulated IDEs.

Visual inspection showed that the single uncoated Cu IDE with reduced impedance was exhibiting verdigris, on the copper surface, with corrosion products precipitated between tracks at the FR4-silicone interface, Fig. 8. On inspection other uncoated Cu IDEs were observed to have dark copper(II) oxide at the copper surface, Fig. 8.

C. Moisture Absorption

Following soaking in deionized water for 168 hours the change in bare FR4-Cu laminate sample mass was 1.0059 ± 0.0007 relative to dry mass (unitless, calculated as $\text{mass}_{\text{wet}} / \text{mass}_{\text{dry}}$) and silicone encapsulated sample mass was 1.0034 ± 0.0014 . FR4-Cu laminate absorbed $0.59 \pm 0.07\%$ moisture by mass, and silicone $0.34 \pm 0.14\%$ moisture by mass. Some variation in moisture absorption was observed over time, Fig. 9.

IV. DISCUSSION

Silicone coated Cu-FR4 IDEs with silicone encapsulation were aged in saline with heat acceleration. Solder coated IDEs were observed to have stable 1 kHz impedance over 330 days including 2 months accelerated aging at 67°C , Fig. 3. Uncoated IDE 1 kHz impedance was observed to vary: most samples showed an impedance increase during 67°C aging which must be investigated further; and a single sample showed an impedance decrease associated with copper oxidation, Fig. 8. Copper oxidation in the single uncoated sample appears similar to the failure observed within a prototype implant continually operated for 15 days at 100°C , Fig. 1. We hypothesise that the observed verdigris and copper(II) oxide formation is due to moisture ingress into voids due to FR4 porosity or at the Cu-FR4-silicone interface at the edge of copper tracks, local corrosion and resulting osmotic pressure led to FR4-silicone delamination and leakage paths between the electrodes and a reduction in impedance [4]. We observed that both FR4-Cu laminates and silicones absorb water and this can be expected to change the dielectric properties and therefore IDE impedance. Sectioning and elemental analysis of failed and as produced samples will be essential to check for the presence of voids at the FR4-Cu interface and for contaminants and corrosion products. The observed verdigris is also attributable to insufficient surface cleaning [6], where contaminants act as a water nucleation

point, and indicates the presence of chloride, sulphate or carbonate ions. Solder coating achieved increased IDE lifetimes with no failures apparent and is therefore promising for pre-clinical prototype implants where short device lifetimes (months) are required, for example for basic neuroscience. The survival of solder coated IDEs does not support the hypothesis of failure due to FR4 porosity, which would still be present beneath the copper layer, instead the solder may cover and smooth pinholes or other irregularities in the copper surface which are not filled during silicone encapsulation. Silicone rubber is a promising material due to its observed adhesion to FR4 [9]. However, alternative encapsulation methods can provide sufficient lifetimes for pre-clinical prototype active implants including epoxies, parylene C, polyimide, and liquid crystal polymers [2,12].

ACKNOWLEDGMENT

The authors thank N. Donaldson for equipment access.

REFERENCES

- [1] H. T. Lancashire, M. Habibollahi, D. Jiang, and A. Demosthenous, "Evaluation of Commercial Connectors for Active Neural Implants," in *2021 10th International IEEE/EMBS Conference on Neural Engineering (NER)*, May 2021, pp. 973–976. doi: 10.1109/NER49283.2021.9441072.
- [2] T. Stieglitz, "Implantable Device Fabrication and Packaging," in *Handbook of Neuroengineering*, N. V. Thakor, Ed., Springer Nature, 2023, pp. 289–337. doi: 10.1007/978-981-16-5540-1_102.
- [3] R. Traeger, "Nonhermeticity of Polymeric Lid Sealants," *IEEE Transactions on Parts, Hybrids, and Packaging*, vol. 13, no. 2, pp. 147–152, Jun. 1977, doi: 10.1109/TPHP.1977.1135193.
- [4] A. Vanhoestenberghé and N. Donaldson, "Corrosion of silicon integrated circuits and lifetime predictions in implantable electronic devices," *J. Neural Eng.*, vol. 10, no. 3, p. 031002, May 2013, doi: 10.1088/1741-2560/10/3/031002.
- [5] P. E. K. Donaldson, "The essential role played by adhesion in the technology of neurological prostheses," *International Journal of Adhesion and Adhesives*, vol. 16, no. 2, pp. 105–107, May 1996, doi: 10.1016/0143-7496(95)00031-3.
- [6] P. Kiele, J. Hergesell, M. Bühler, T. Boretius, G. Suaning, and T. Stieglitz, "Reliability of Neural Implants—Effective Method for Cleaning and Surface Preparation of Ceramics," *Micromachines*, vol. 12, no. 2, Art. no. 2, Feb. 2021, doi: 10.3390/mi12020209.
- [7] D. Jiang *et al.*, "A Versatile Hermetically Sealed Microelectronic Implant for Peripheral Nerve Stimulation Applications," *Frontiers in Neuroscience*, vol. 15, 2021, doi: 10.3389/fnins.2021.681021.
- [8] L. Lonys *et al.*, "Design and implementation of a less invasive gastrostimulator," *European Journal of Translational Myology*, vol. 26, no. 2, Art. no. 2, Jun. 2016, doi: 10.4081/ejtm.2016.6019.
- [9] L. Lonys *et al.*, "Silicone rubber encapsulation for an endoscopically implantable gastrostimulator," *Med Biol Eng Comput.*, vol. 53, no. 4, pp. 319–329, Apr. 2015, doi: 10.1007/s11517-014-1236-9.
- [10] A. Carnicer-Lombarte, H. T. Lancashire, and A. Vanhoestenberghé, "In vitro biocompatibility and electrical stability of thick-film platinum/gold alloy electrodes printed on alumina," *J Neural Eng.*, vol. 14, no. 3, p. 036012, Jun. 2017, doi: 10.1088/1741-2552/aa6557.
- [11] N. Donaldson, C. Lamont, A. S. Idil, M. Mentink, and T. Perkins, "Apparatus to investigate the insulation impedance and accelerated life-testing of neural interfaces," *J. Neural Eng.*, vol. 15, no. 6, p. 066034, Oct. 2018, doi: 10.1088/1741-2552/aadeac.
- [12] S. L. C. Au, F.-Y. B. Chen, D. M. Budgett, S. C. Malpas, S.-J. Guild, and D. McCormick, "Injection Molded Liquid Crystal Polymer Package for Chronic Active Implantable Devices With Application to an Optogenetic Stimulator," *IEEE Transactions on Biomedical Engineering*, vol. 67, no. 5, pp. 1357–1365, May 2020, doi: 10.1109/TBME.2019.2936577.